

Fog detection through full exploitation of satellite observations using machine learning



Böhm¹, C. and S. Crewell¹

¹ Institute of Geophysics and Meteorology, University of Cologne

1. Introduction

Fog affects human life and various ecosystems as well as the climate system. For a better understanding of the underlying mechanisms, more accurate observations are required. State-of-the-art satellite-based approaches, which can provide sufficient spatial coverage, suffer from limited detection skill and a bias towards certain fog types under specific atmospheric and surface conditions. Machine learning opens up new research pathways exceeding the capabilities of conventional methods.

The Atacama Desert is most suitable to develop satellite-based fog retrievals being frequently affected by fog and exhibiting constant background emissivity due to the lack of lush vegetation. Ground-based references are provided by weather stations built by the Collaborative Research Center 1211 (Dunai et al. 2020). We develop novel fog retrievals to study fog behavior under the following objectives:

1. Build algorithms which exploit spectral channels (Böhm et al. 2021) and spatial features
2. Identify fog characteristics via explainable ML
3. Determine spatiotemporal fog variability

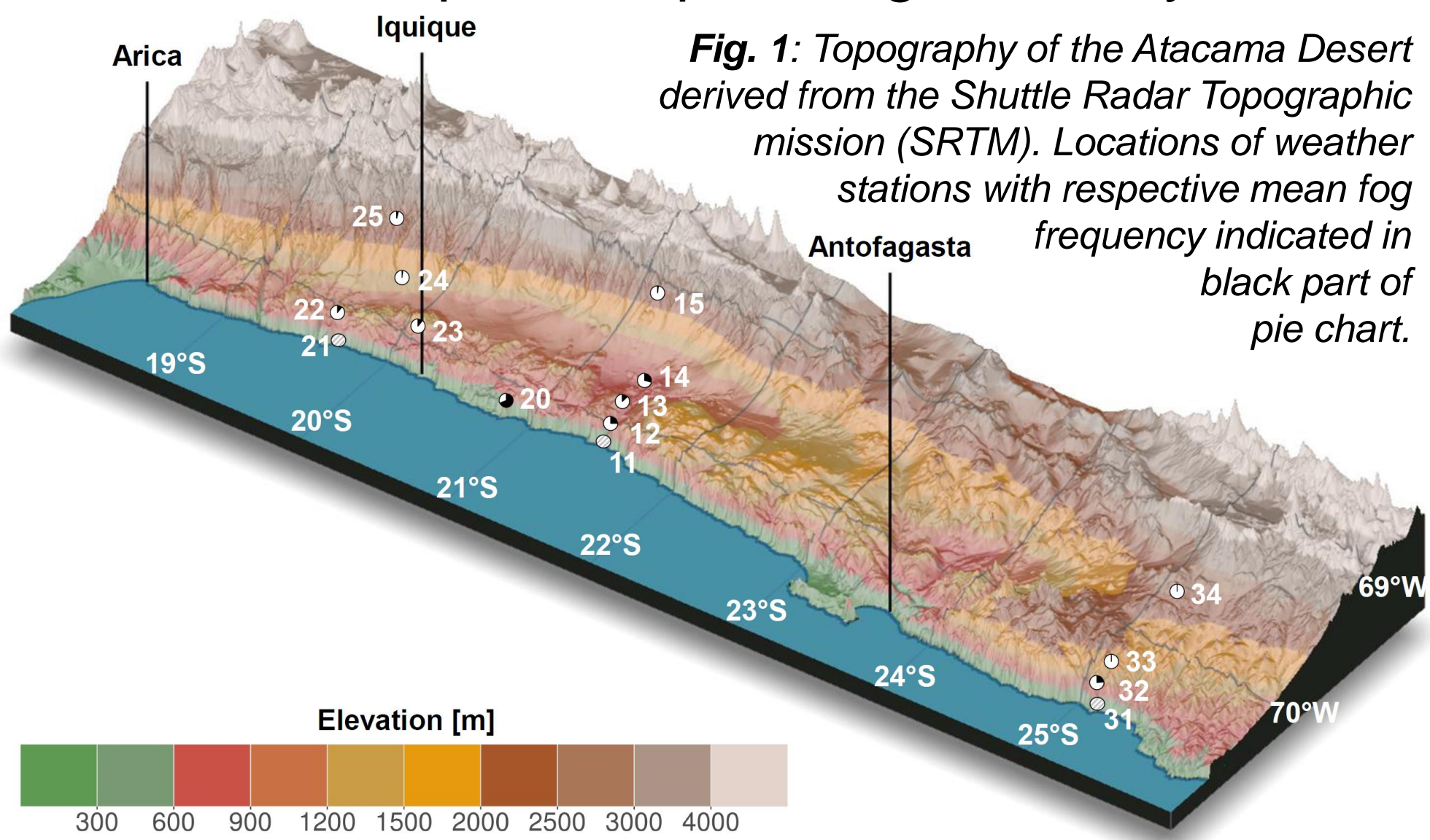


Fig. 2: Photos of a) coastal morning fog near station 13 (29 June 2017, 9:00 LT) and b) Tillandsia dune at Cerro Oyarvide within coastal fog ecosystem (Jaeschke et al. 2019).

2. Data

Platform/instrument	Period	Description and utilized channels
Ground-based weather stations	2017-present	Measurements of Leaf Wetness Sensor voltage U , relative humidity rh , temperature at 2m and surface with $\Delta\theta = \theta_{2m} - \theta_{surf}$, longwave radiation budget ΔP (Schween et al. 2020)
Moderate Resolution Imaging Spectroradiometer (MODIS) on Terra and Aqua satellites	2002-present	1km nadir resolution; polar orbit; overpasses ~ 23h and 2h (LT) 15 thermal emissive bands (3.75–14 μ m) spectral radiances from level-1B Calibrated Radiances Product (MOD021KM, MYD021KM; MODIS Characterization Support Team 2017)
Advanced Baseline Images (ABI) on the Geostationary Operational Environmental Satellite (GOES)	2018-present	2 km nadir resolution; geostationary; temp. resol. 10 to 15 min 10 emissive bands (3.75–13.3 μ m), 6 visible (0.47–2.26 μ m) brightness temperatures, reflectances data source: Andi Walther, SSEC, University of Wisconsin

3. Ground-based fog retrieval

- state of leaf wetness sensor
- refined based on additional measurements to account for adjustment time at begin and end of fog episodes
- suitable thresholds derived via self-organizing maps (SOMs)

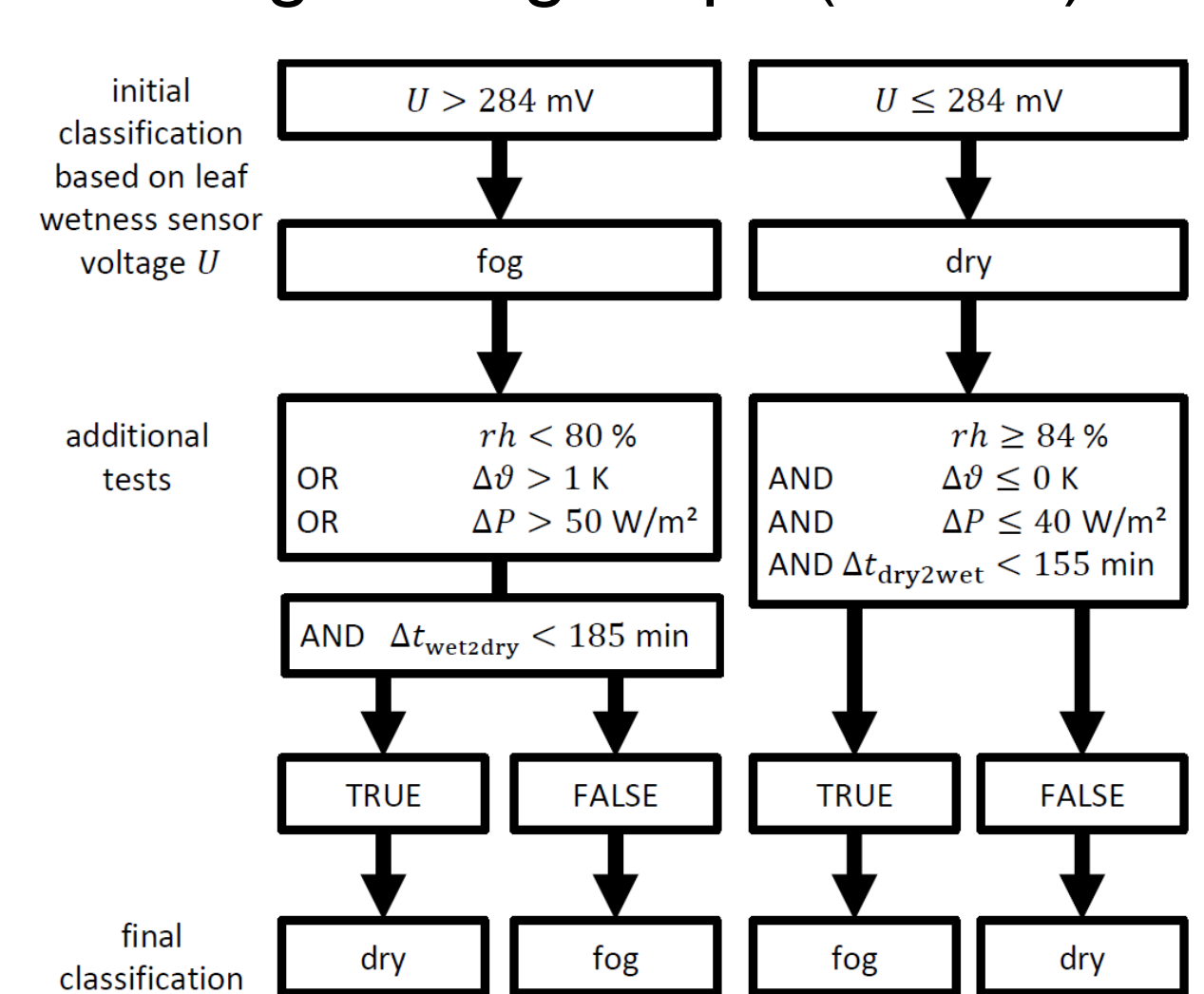


Fig. 4: Ground-based fog classification scheme. Thresholds used to refine an initial classification based on the leaf wetness sensor voltage were derived by visual inspection of the SOMs.

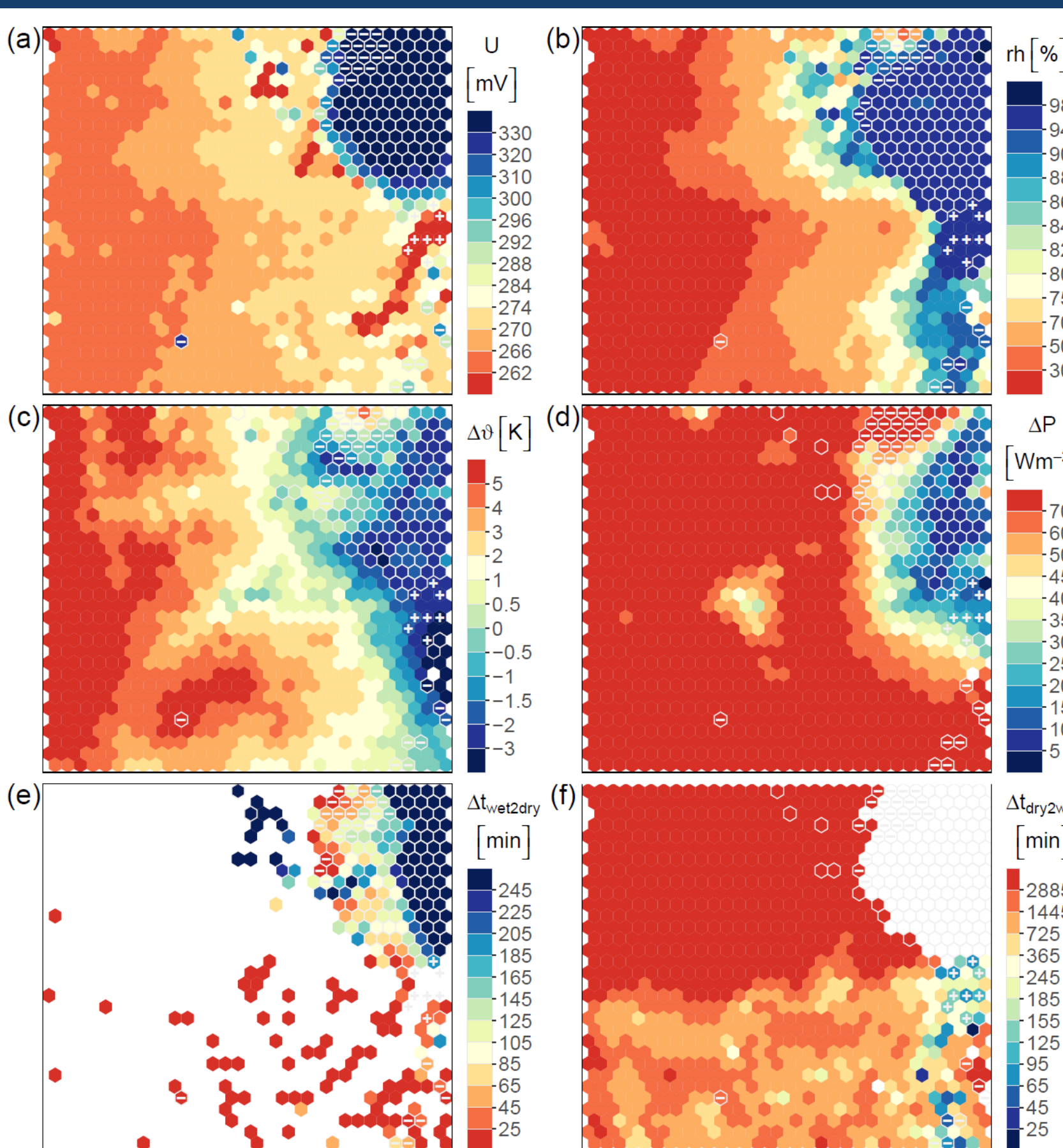
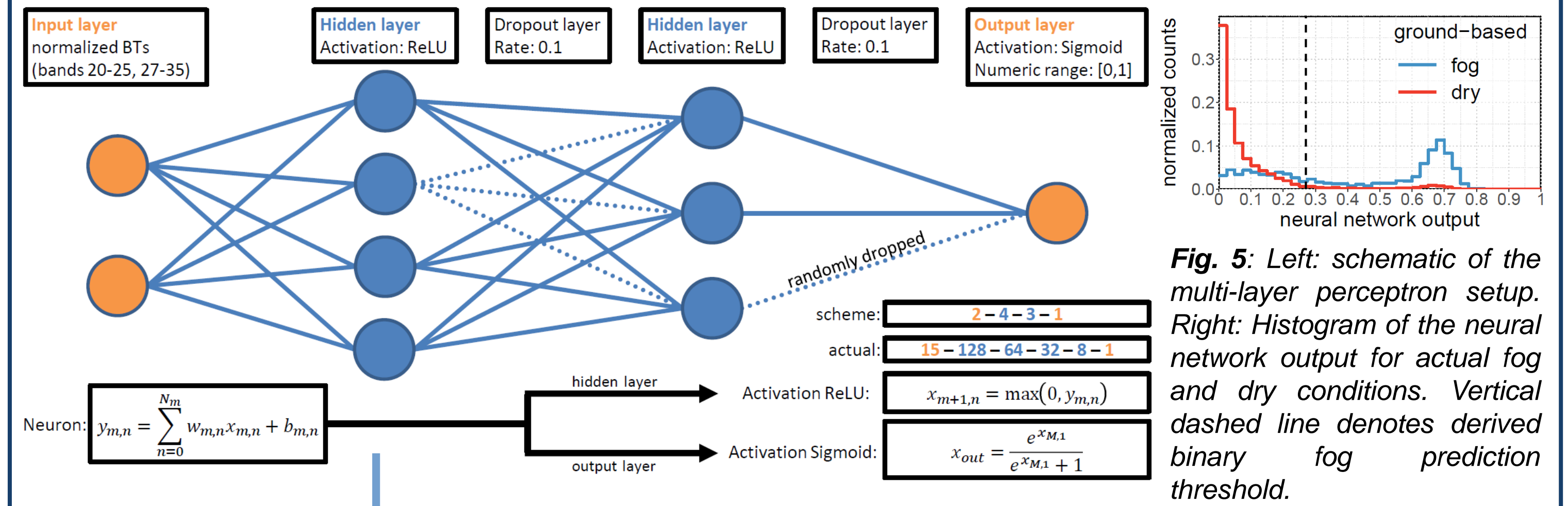


Fig. 3: SOM for climate station 13. Value ranges that typically coincide are displayed in the same region of each map. $\Delta t_{wet2dry}$: time until a wet leaf wetness sensor switches to dry, $\Delta t_{wet2dry}$ vice versa. White frames: sensor is wet. +/-: dry/wet classification flipped.

4. Fog from spectral dimension – MODIS (Böhm et al. 2021)



- attempt to distinguish low clouds and fog by training with ground-based fog data
- accuracy: 0.89; probability of detection: 0.63; false alarm rate: 0.37; Heidke Skill Score: 0.56 for independent test data → comparable skill with state-of-the-art approach derived for Europe (Egli et al. 2018)
- time series correlation betw. neural network output and ground-based fog on for 60-day mov. avg. betw. 0.75–0.9 → suitable representation of temporal variability
- similar correlation when respective stations are left out from training → region-wide generalization

- region-wide quantification of fog frequency
- coastal fog corridors higher resolved than ever before
- fog spots in central valley of the Atacama discovered

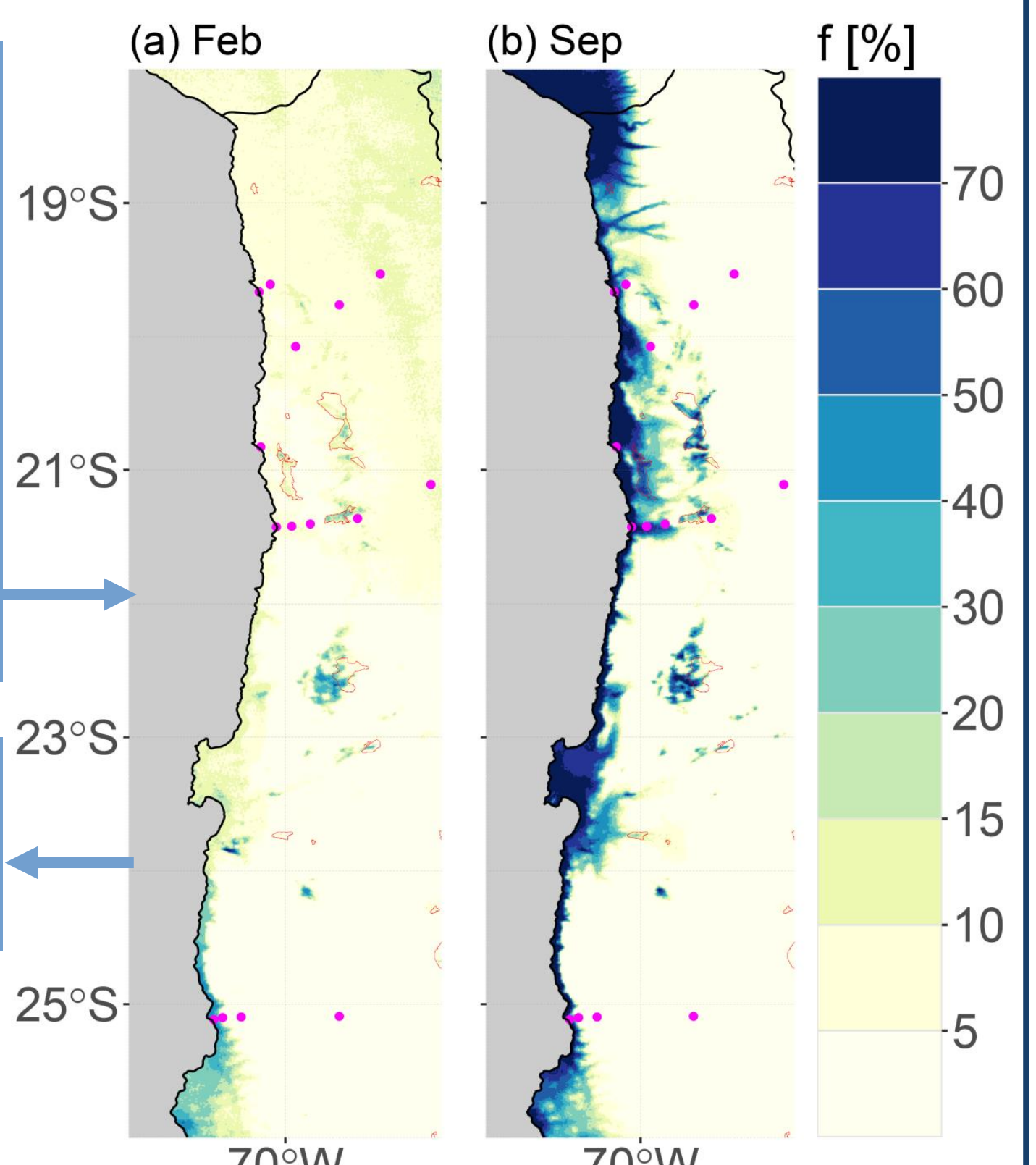
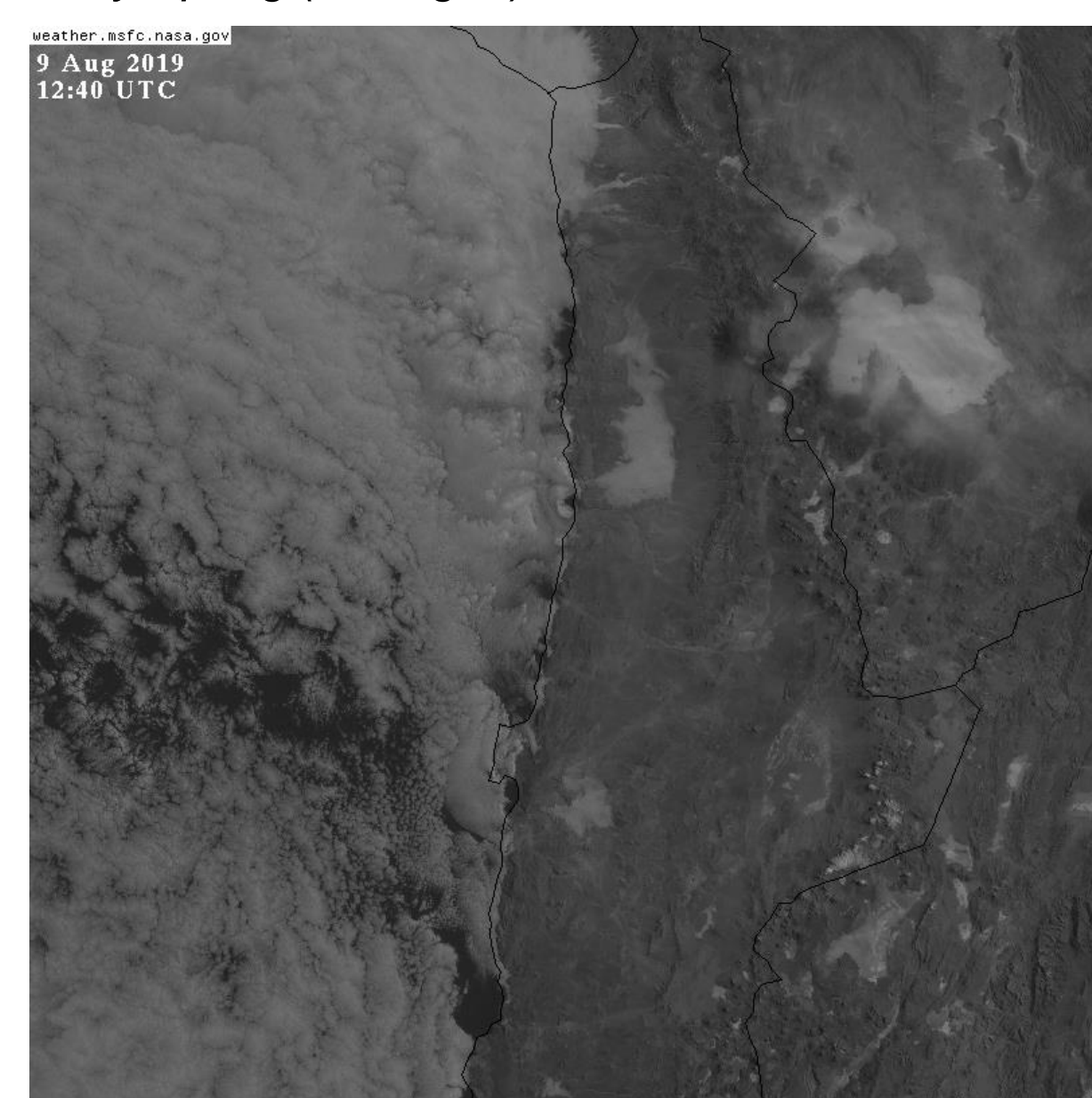


Fig. 6: 19-year climatology of nocturnal fog frequencies (23h and 2h overpasses betw. 2003–2021) for (a) February (lowest coastal fog freq.) and (b) September (highest coastal fog freq.). Magenta dots: Ground-based stations. Red contour: salt flats.

5. Fog from spectral and spatial dimensions – GOES

Fig. 7: GOES visible image for 9 August 2019 at 8:40 LT. The residuals of fog which formed during the preceding night can be seen in the central valley. Fog occurrence in this region is typical for early Spring (c.f. Fig. 6).



Outlook:

- cover full diurnal cycle by applying geostationary image data (GOES)
- exploit spatial fog features and textures by processing whole images
- efficient image segmentation via U-Net architecture (Ronneberger et al. 2015, Dröchner et al. 2018)

Challenges:

- training with limited annotations (climate stations)
 - train with different image crops
 - randomize annotation locations (Wang et al. 2020)
- daytime and twilight situations → varying solar component for NIR channels
 - train only with thermal emissive channels (e.g. Andersen and Cermak 2018)
 - Tune network to produce diurnally consistent bias and RMSE

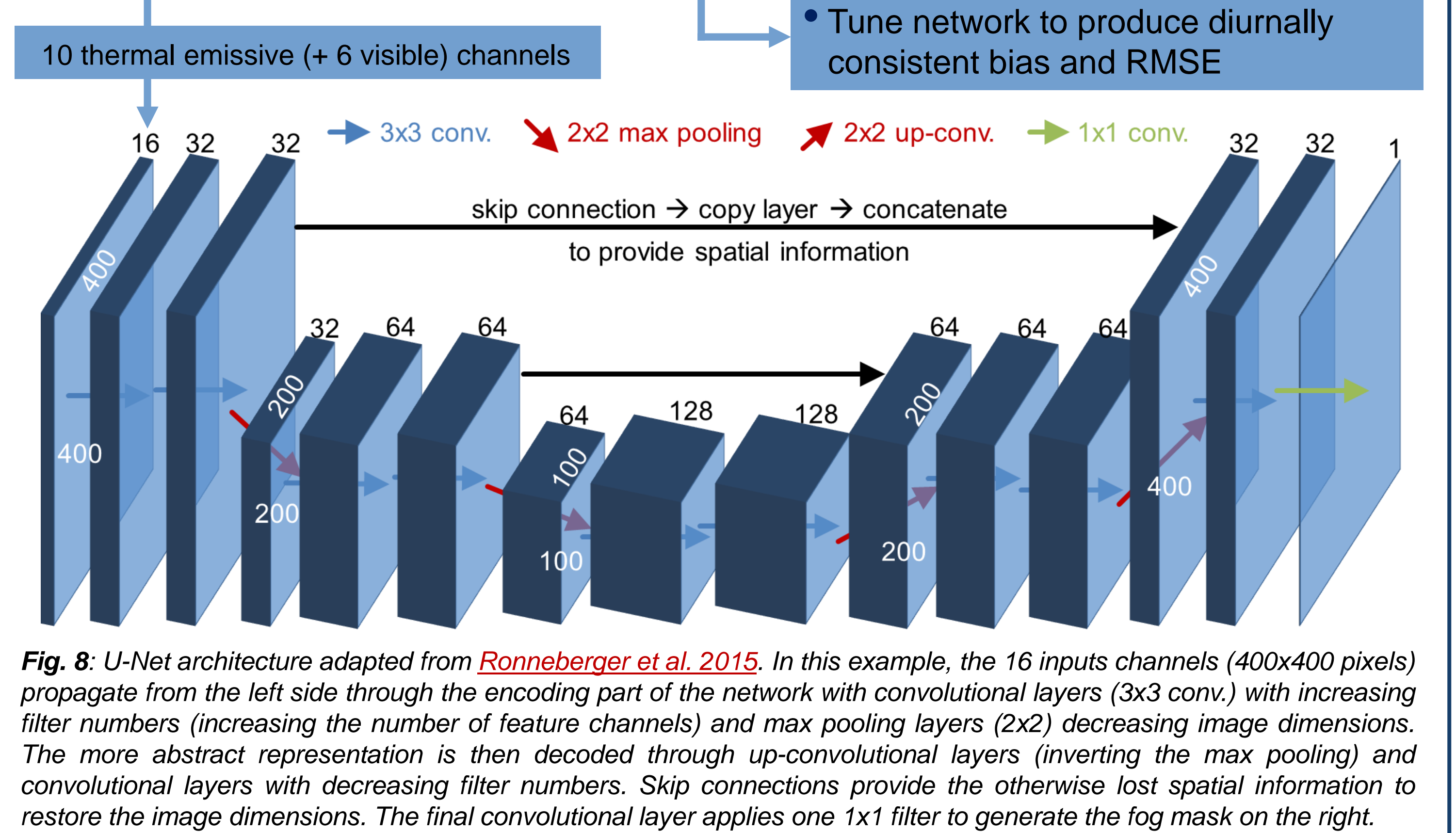


Fig. 8: U-Net architecture adapted from Ronneberger et al. 2015. In this example, the 16 inputs channels (400x400 pixels) propagate from the left side through the encoding part of the network with convolutional layers (3x3 conv.) with increasing filter numbers (increasing the number of feature channels) and max pooling layers (2x2) decreasing image dimensions. The more abstract representation is then decoded through up-convolutional layers (inverting the max pooling) and convolutional layers with decreasing filter numbers. Skip connections provide the otherwise lost spatial information to restore the image dimensions. The final convolutional layer applies one 1x1 filter to generate the fog mask on the right.

References: Dunai et al., 2020, DOI:10.1016/j.gloplacha.2020.103275; Böhm et al., 2021, DOI:10.1175/JAMC-D-20-0208.s1; Jaeschke et al., 2019, DOI:10.1016/j.gloplacha.2019.103029; MODIS Characterization Support Team, 2017, DOI:10.5067/MODIS/MOD021KM.061; Egli et al., 2018, DOI:10.3390/rs10040628; Ronneberger et al., 2015, DOI:10.1007/978-3-319-24574-4_28; Dröchner et al., 2018, DOI:10.3390/rs10111782; Wang et al., 2020, DOI:10.3390/rs12020207; Andersen and Cermak, 2018, DOI:10.5194/amt-11-5461-2018